



Electro-Responsive Green Gels for Lower Environmental Impact Shale Gas Extraction

This is the peer reviewed version of the following article:

Original:

Sarri, F., Tatini, D., Raudino, M., Ambrosi, M., Carretti, E., Lo Nostro, P. (2019). Electro-Responsive Green Gels for Lower Environmental Impact Shale Gas Extraction. ENERGY & FUELS, 33(3), 2057-2066 [10.1021/acs.energyfuels.8b04321].

Availability:

This version is available <http://hdl.handle.net/11365/1285194> since 2025-01-30T10:10:23Z

Published:

DOI:10.1021/acs.energyfuels.8b04321

Terms of use:

Open Access

The terms and conditions for the reuse of this version of the manuscript are specified in the publishing policy. Works made available under a Creative Commons license can be used according to the terms and conditions of said license.

For all terms of use and more information see the publisher's website.

(Article begins on next page)

ELECTRO-RESPONSIVE GREEN GELS FOR LOWER ENVIRONMENTAL IMPACT SHALE GAS EXTRACTION

*Filippo Sarri^a, Duccio Tatini^a, Martina Raudino^a, Moira Ambrosi^a, Emiliano Carretti^a,
Pierandrea Lo Nostro^{a,b*}*

a: Department of Chemistry “Ugo Schiff” & CSGI, University of Florence, 50019 Sesto
Fiorentino (Firenze), Italy

b: Enzo Ferroni Foundation, 50019 Sesto Fiorentino (Firenze), Italy

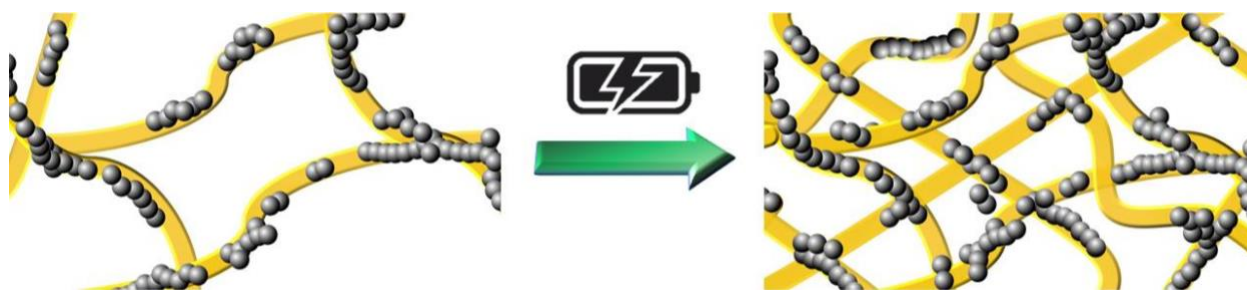
* Email: pierandrea.lonostro@unifi.it

KEYWORDS: green frac fluid; carbon black; electric responsiveness; rheology; smart device;
viscoelastic.

ABSTRACT: In this work, carbon black (CB) is added in small amounts (3-10% w/w) to green aqueous dispersions based on sodium oleate, guar gum, sodium hyaluronate or hydroxypropyl cellulose gels to enhance their stability against mechanical and thermal stresses and provide an electric responsiveness to an external voltage. Rheology, optical microscopy, small angle X-ray scattering, and conductivity measurements are performed to compare the properties of carbon black-enriched formulations to those of the pristine dispersions. Our results demonstrate that

even small amounts of carbon black are able to confer interesting physico-chemical properties to these formulations: a remarkable increase of the viscosity of at least one order of magnitude is observed for all systems even at high temperature (up to 60° C) upon CB addition indicating that carbonaceous particles play a structuring role for the polymeric network. Furthermore, the application of an external voltage of 30 V for 60 mins to CB-containing formulations imparts a significant electric responsiveness to the systems allowing to modify their rheological behavior. The CB-loaded formulations can be recycled at least three times. All these results suggest that the carbon black can be effectively used as an alternative green additive to enhance the mechanical and thermal stability of the formulations and that its addition can be a feasible way to easily tune the properties of viscoelastic materials avoiding the use of toxic or potentially dangerous chemicals. The possibility of achieving the remote control of mechanical and thermal properties of viscoelastic formulations significantly expand the horizon of their potential applications, for example in the field of shale gas extraction.

ABSTRACT GRAPHIC



SYNOPSIS

Electric responsiveness is imparted to green viscoelastic aqueous dispersions used as fracturing fluids by small amounts of carbon black.

1. INTRODUCTION

Shale gas is natural gas (mainly methane and ethane) trapped within shale formations.¹ Shale is a sedimentary rock formation that contains clay, quartz and other minerals depending on the basin. Shale reservoirs do not naturally have sufficient permeability to allow the oil and gas to flow at commercially exploitable rates.² In order to overcome this limitation, a specific process was developed to increase the effective permeability through the creation of high conductivity channels in the form of fractures within the formation. This process is called Hydraulic Fracturing (or “Fracking”), and consists in the high-pressure injection of a 'fracking fluid' into a wellbore to create cracks in the deep-rock formations.³ Shale gas extraction and production are usually associated to some severe environmental issues, *e.g.* the production of wastewater, the contamination of deep fresh groundwater, and the leaking of toxic chemicals on site. There is a great demand for green alternatives, both for products and for processes, aiming at reducing or removing the chemical hazards. Clearly some physical and physico-chemical properties of the frac fluids are crucial for the optimization of their performances *in situ*.

The control of frac fluids viscosity is a key parameter in determining the overall efficiency of the gas extraction process.^{4,5} During the initial stages of the fracturing operations, the formulation viscosity must be appropriately high in order to ensure a correct proppant transport and avoid its sedimentation, which may cause the blockage of the well. When the well is depressurized after fracturing the fluid must lose viscosity and clean up quickly from the

fracture, allowing an efficient recovery and an effective gas extraction.⁶ For polymer-based formulations, which represent the most widely used fracturing fluid systems, the initial increase in the fluid viscosity is generally achieved through the addition of cross-linking agents, such as boric acid, boron derivatives, Ti(IV), Zr(IV), and Al(III) complexes.^{5,7,8} At the end of the fracturing process, specific breakers including oxidizers (ammonium persulfate, sodium persulfate, and calcium and magnesium peroxides) or enzymes (hemicellulase, cellulase, amylase and pectinase) are added to the frac fluid in order to degrade the polymer and induce a viscosity breakdown.^{9,10} Other additives like acids, friction reducers, surfactants, clay control agents, scale inhibitors, pH adjusting agents, iron control agents, corrosion inhibitors, and biocides are also included at low concentrations to impart specific properties to the frac fluids, depending on the reservoir conditions.⁵ Nevertheless, the environmental concerns related to shale gas extraction (*i.e.* wastewater production, groundwater contamination, induced seismicity and greenhouse gas emissions) cast doubts on the toxicity of the chemicals which are present in fracturing fluids.¹¹⁻¹³

The demand for green alternatives, where the toxic and polluting controlled substances are replaced by environmentally-friendly and biocompatible materials, the recovery of frac fluids, the re-use of flowback and produced water, and the limitation of the extracted NORM (Naturally Occurring Radioactive Materials) prompt several researchers to explore new innovative approaches for fracturing fluid formulations. The industry is focused on the development of alternative polymers that can replace guar gum, due to occasional high prices and short supply, as well as public concerns about fresh water supplies.⁵ At the same time, several efforts have been made to develop environmentally- and equipment-friendly additives that can be applied at high temperatures and extremely low or high pH conditions.^{14,15} Other research directions

include the development of slickwater systems that can use less or no water, the formulation of hydraulic fracturing fluids by recycling produced water with a high salinity content, the improvement of viscoelastic surfactant (VES)-based fluids to be compatible with high salinity-produced water, divalent ions in formations as well as high temperature environments, and the development of “energized fluids” based on CO₂ and nitrogen with enhanced proppant transport capability.^{5,16–18} A very promising approach for the formulation of a new generation of frac fluids is the design of *stimuli*-responsive systems, whose rheological and mechanical properties can undergo controlled and reversible modifications in response to an external *stimulus*.^{19,20} The stimulus or external field applied include thermal, electric, magnetic, pH, UV/visible light, ionic or metallic interactions or combinations thereof.^{21,22} For gas and oil applications, the most investigated systems are thermo- and salt-responsive materials, since their rheological behavior can be effectively modulated using the intrinsic variations of temperature and salt composition inside the formations.¹⁹ The need for a clear-cut control on the fluid modifications lead to the development of more efficient systems, which respond to different chemical *stimuli*. Jung *et al.* reported a switchable hydraulic fracturing fluid that undergoes a reversible, large and fast volume expansion triggered by CO₂ with a simultaneous increase in viscosity.²³ A similar strategy is followed by Zhang *et al.* for the development of a viscoelastic surfactant-based nanostructured fluid that responds to specific *stimuli*, namely pH and CO₂ gas, switching between a high viscosity wormlike micellar network and a low-viscosity dispersion with precipitate.²⁴

In this work we developed a system for the modulation of frac fluid viscosity through a physical *stimulus* (*i.e.* an applied voltage), which overcomes all the limitations related to chemical triggers, such as the irregular fluctuations in the chemical composition and pH

conditions of flowback water during the drilling/extraction operations, or the addition of specific chemicals to the fracturing fluid. In particular, we investigated the effect of relatively small amounts of carbon black (CB) on the electroresponsiveness and the thermal and rheological properties of two different classes of aqueous frac fluid formulations. The first was a linear gel system based on a polysaccharide dispersion in water, *i.e.* guar gum (GG), sodium hyaluronate (SH) and hydroxypropyl cellulose (HPC). The second system was a viscoelastic surfactant-based (VES) formulation containing a green anionic surfactant (sodium oleate, NaOL) as the main ingredient in combination with an inorganic salt (potassium chloride). Carbon black was added to these formulations in relatively small amounts, namely 3% and 10% w/w for polysaccharides and VES formulations, respectively. It is worth noting that such CB contents are much lower than 20% w/w, which is the amount of carbon black or carbon nanotubes commonly used to modify the properties of most composites.²⁵ CB is an anthropogenic carbonaceous material that is essentially a pure form of soot, produced during an incomplete combustion of hydrocarbons.²⁶ Different manufacturing processes produce different types of carbon black, including furnace black, thermal black and conduct black. CB is extensively used as filler in the rubber industry to prepare composites with improved strength, stiffness and wear resistance properties.²⁷ CB also finds a remarkable use in the polymer industry, especially in the production of polypropylene, polyvinyl chloride, polyester and polyethylene.^{28–30} The presence of carbonaceous particles confers an enhanced electric conductivity and an increased resistance to thermal degradation, abrasion and tear to the polymer matrix.³¹ Moreover, the addition of CB brings about other advantages, *i.e.* the reduction of the amount of polymeric materials (with no significant modification in their mechanical properties) and the reinforcement of the polymer viscoelastic behavior.³² Several theories, such as tunneling and percolation models, have been developed in

the past to explain how the presence of CB affects the mechanical and rheological behavior of these composite materials.^{33–36} Steric, electrostatic, excluded volume and hydrogen bonding interactions rule over the thermal, mechanical and rheological behavior of such systems since they are composed of a solid and rigid matrix where polymer chains and carbon black particles are in direct contact. In our case, the scenario is totally different since the dispersed polysaccharides or viscoelastic surfactants are free to diffuse in the continuous aqueous phase containing also CB particles. This feature certainly modifies the intermolecular interactions between the ingredients of these multicomponent systems, that include solvation, steric and hydrophobic effects and depletion forces. Further experiments should be performed to investigate this topic more thoroughly.

The effect of CB on the frac fluids' properties was investigated by means of rheology (flow curves and oscillatory measurements), electric stimulation experiments, optical microscopy, and small angle X-ray scattering (SAXS) experiments. The results suggest that CB improves the performances of such water-based dispersions without affecting the 3D ordered network and its rheological behavior. The application of a moderately low voltage to the CB-enhanced frac fluid formulations results in a prompt collapse of the gel structure with a consequent viscosity breakdown. The process is reversible as the frac fluids can be recovered and recycled. Moreover, the addition of carbon black enhances the thermal resistance of the formulation preventing the viscosity loss at high temperature.

The formation of fluid systems that contain relatively moderate amounts of CB paves the way to new potential applications in so far unexplored fields, such as the formulation of green fluids for hydraulic fracturation involved in a lower environmental impact of shale gas extraction.

2. EXPERIMENTAL SECTION

Materials. Sodium oleate (ACS grade) was purchased from Riedel-De Haën (Seelze, Germany). Carbon Black VULCAN[®] XC-72R was provided by Cabot Corporation (Boston, USA), KCl ($\geq 99\%$) and saponin ($\geq 99\%$) were purchased from Sigma-Aldrich (Milan, Italy), guar gum and hydroxypropyl cellulose (average molecular mass 2000 and 1600-1800 kDa, respectively) were supplied by Lamberti S.p.A. (Milan, Italy), and high molecular weight (1800 – 2000 kDa) sodium hyaluronate was purchased from Stanford Chemicals Company (Fairbanks, CA). All solutions and dispersions were prepared with Milli-Q water (resistivity $> 18 \text{ M}\Omega \cdot \text{cm}$ at $25 \text{ }^\circ\text{C}$).

Preparation of polysaccharide-based formulations. 0.5% w/w water dispersions of guar gum (GG), hydroxypropyl cellulose (HPC) and sodium hyaluronate (SH) were prepared by slowly adding a weighed amount of the polysaccharide powder to MilliQ water under constant stirring at room temperature. In these conditions homogeneous dissolution occurs in about 30 minutes for all the investigated biopolymers thus giving homogeneous and transparent samples, except for guar gum dispersions which appear slightly cloudy due to the presence of seeds' residues in the commercial material. All samples remain transparent after their preparation at least up to 12 months.

Preparation of VES formulations. VES frac fluids were prepared by dissolving under magnetic stirring the proper amount of sodium oleate in MilliQ water or in a 0.5 M (4% w/w) KCl aqueous solution in order to obtain a final surfactant concentration of either 2% or 13% w/w.

Preparation of Carbon Black-enhanced frac fluids. Carbon black was added to the polysaccharide or to the VES samples following two different procedures: a) To effectively include CB in the polysaccharide matrices, a 2% w/w saponin solution was first prepared. Saponins belong to a class of natural surfactants which are effectively used to stabilize carbonaceous particles in water dispersions.^{37,38} This solution was added to a weighed amount of CB in order to obtain a final CB concentration of either 1% or 3% w/w and magnetically stirred for a few minutes. The mixture was sonicated for 1 hour at 40 kHz and the polysaccharide was added under magnetic stirring. b) In the case of the VES systems, no additive was necessary for the dispersion of CB, as sodium oleate itself is able to disperse the carbonaceous particulate. Hence, the VES solution (NaOL 13% + KCl 0.5 M) was simply added to a weighed amount of CB (1, 3 or 10% w/w), then the mixture was sonicated for 30 minutes. Rheology tests were carried out and showed that the formulations retain their original rheological properties after the addition of CB and sonication.

Optical Microscopy. Nikon Eclipse Ti-S Inverted Microscope was used to obtain optical images of CB dispersions in saponin and sodium oleate. All experiments were performed in automatic mode using an objective with a 10x magnification at room temperature. At least three different regions for each sample were analyzed in order to obtain a statistically meaningful result.

Flow Curves of Polysaccharide and VES Systems. Rheological measurements were performed with a Paar Physica UDS 200 rheometer working in the controlled shear-stress mode. For all samples a plate–plate geometry (diameter 4.0 cm; gap 300 μm) was used. In these operating conditions, the total amount of the sample in the cell was about 0.5 mL, and the temperature was set at 25, 30, 40, 50 or 60 °C with a Peltier control system. For each sample, the flow curve was acquired in a torque range between 10^{-3} and 2000 mN·m, after a 15 minutes soaking time to equilibrate at the set temperature.

Frequency Sweep on VES Formulations. Frequency sweep measurements were carried out within the linear viscoelastic range determined by means of an amplitude sweep test. The storage (G') and loss (G'') moduli were measured over the frequency range of 0.001 to 100 Hz.

Electric Responsiveness. The electric responsiveness of VES and polysaccharide-based systems was assessed by applying a 30 V voltage for 1 hour through a Hewlett Packard Harrison 6112 A DC power supply. Two platinum wires of 1.0 mm diameter (Sigma-Aldrich) were dipped into the dispersions and used as electrodes (See Figure 1).

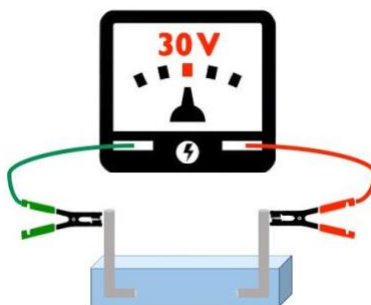


Figure 1. Schematic representation of the setup for the electric treatment.

The applied voltage induces a phase separation in the frac fluid formulations; the two phases that concentrate at the cathode and at the anode are recovered (taking advantage of their different viscosities) and weighed.

SAXS Experiments. SAXS experiments were carried out using a HECUS S3-Micro (Kratky camera) equipped with two position-sensitive detectors (PSD-50M) containing 1024 channels of 54- μm width. Cu $K\alpha$ radiation of wavelength 1.542 Å was provided by a GeniX X-ray generator (Xenocs, Grenoble) working with a microfocus sealed-tube operating at 50 W. The sample to detector distance was 281 mm. The volume between the sample and the detector was kept under vacuum during the measurements to minimize scattering from the air. The Kratky camera was

calibrated using silver behenate, which is known to have a well-defined lamellar structure ($d = 58.38 \text{ \AA}$).³⁹ Scattering curves were monitored in a q -range from 0.02 to 0.55 \AA^{-1} . Liquid samples were analyzed in a borosilicate glass capillary tube. For all measurements the temperature was kept constant at $25 \text{ }^\circ\text{C}$ controlled by a Peltier element, with an accuracy of $\pm 0.1 \text{ }^\circ\text{C}$. All scattering curves were corrected for the empty capillary contribution considering the relative transmission factors. Desmearing of the SAXS curves was not necessary because of the sophisticated point microfocusing system.

3. RESULTS AND DISCUSSION

Dispersibility of carbon black. Optical micrographs of CB in the presence of saponin and sodium oleate are acquired to assess the dispersibility of carbon black as a function of its concentration (Figure 2). Indeed, it was proved that the structure of carbon black, the nature of the polymer, and the processing history of the sample affect the electric conductivity of the composite.^{40,41}

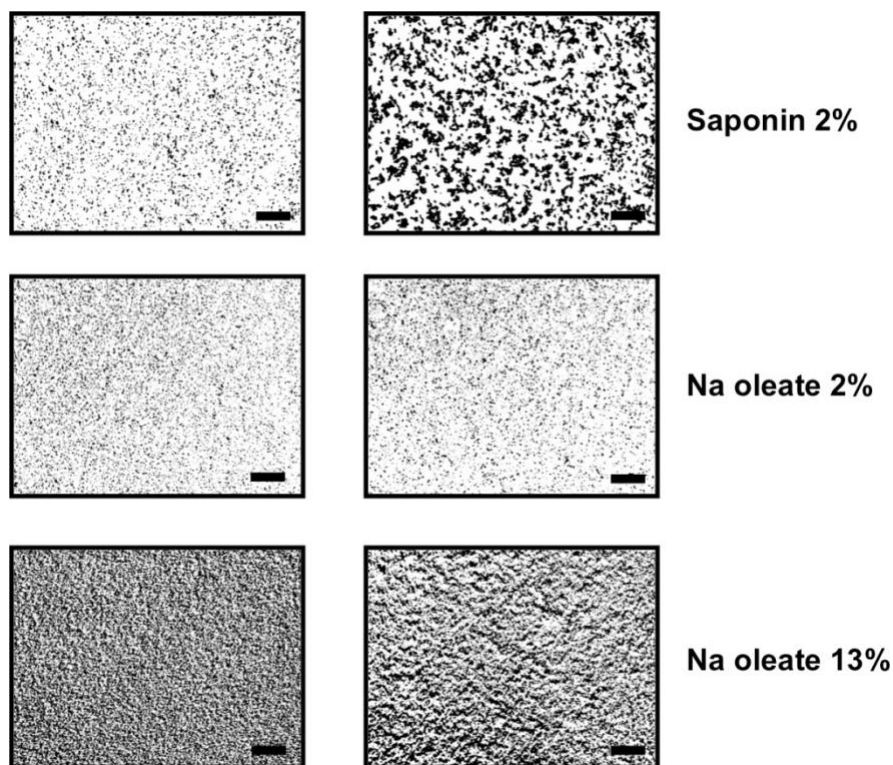


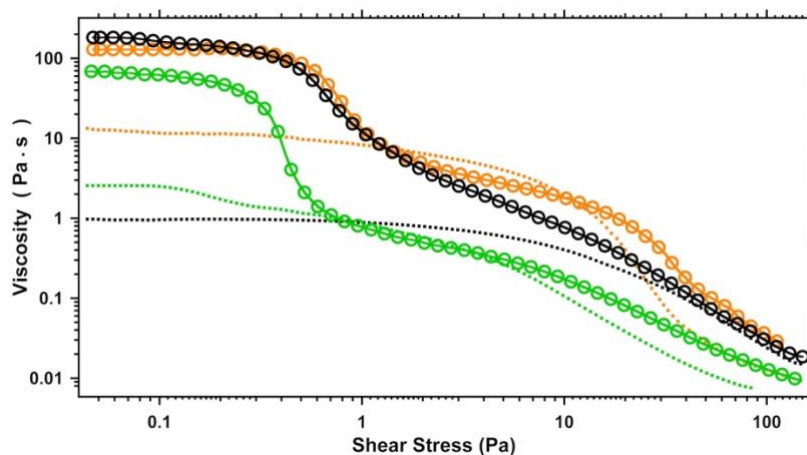
Figure 2. Optical images of carbon black 1% (left) and 3% w/w (right) dispersions in saponin 2% and sodium oleate 2% and 13% w/w. Scale bar: 300 μm .

Stable aqueous dispersions of CB are obtained both with saponin and sodium oleate. The formation of aggregates is observed when the amount of carbon black increases from 1% to 3% w/w, and the carbonaceous particulate appears to be homogeneously dispersed in all samples. Optical micrographs of the CB-enriched polysaccharides and VES-based formulations (see Figure S1 in the Supporting Information) show that carbon black particles are macroscopically homogeneously dispersed into the polymeric/micellar matrices, even at very high CB concentration (10% w/w for the VES fluid), as the visual inspection shows. Therefore, any effect on the electro-responsiveness due to samples inhomogeneity can be disregarded.

This result is of particular interest for practical applications since several efforts were made to find a simple and feasible way to disperse hydrophobic carbonaceous materials, such as fullerenes or carbon nanotubes in aqueous media, especially for biomedical applications.^{42,43} Some works report the encapsulation of CB in silica^{44,45} or polymer particles,⁴⁶ while others suggest the use of surfactant molecules, that can provide both electrostatic and steric stabilization, depending on the nature of the hydrophilic head.^{37,38}

In our samples, saponin adsorbs by exposing its hydrophobic moieties to the CB surface, while the hydrophilic head faces the aqueous phase.³⁸ For sodium oleate, we expect that its adsorption at the CB surface occurs through the C=C double bond in the chain, as suggested by Wang,⁴⁷ while the negatively charged carboxylate provides an electrostatic stabilizing effect.

Rheological behavior. Flow curves are acquired on both pure and carbon black-enriched polysaccharides and VES fluids. The most significant changes are observed for the formulations containing 3 and 10% w/w of CB, respectively. The different rheological profiles are reported in Figure 3.



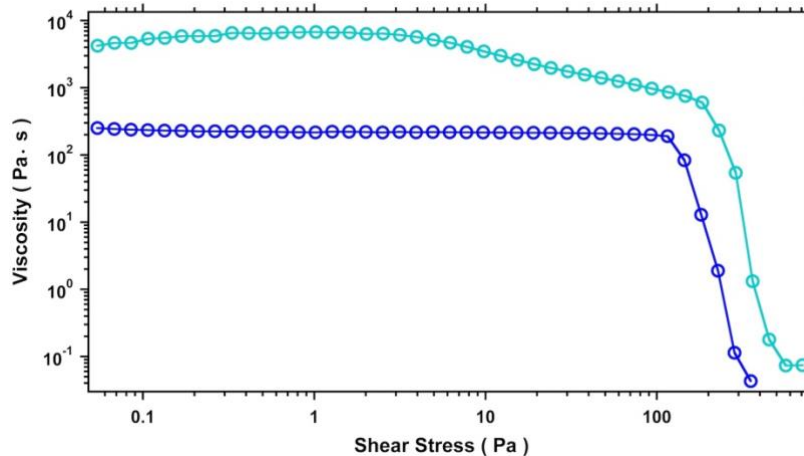


Figure 3. Top: Flow curves of 0.5% w/w pure (dotted lines) and containing 3% w/w of CB (empty circles) GG (green), HPC (black), and SH (orange) dispersions. Bottom: Flow curves of NaOL 13% + KCl 4% (dark blue) and NaOL 13% + KCl 4% in the presence of CB 10% w/w (light blue).

The pure polysaccharide dispersions exhibit a non-Newtonian behavior with the zero-stress viscosity η_0 ranging between 1 and 13 Pa·s moving from HPC to SH. These values are consistent with the viscosities reported for typical linear gel frac fluid formulations.^{7,9} The addition of CB brings about two remarkable effects in the frac fluid rheological behavior: first, it leads to an increase in the viscosity of at least one order of magnitude, which reflects the effective inclusion of the additive in the polysaccharide matrices. Second, the rheological profiles are significantly modified with respect to the pure polysaccharides when CB is added to the formulations. Indeed, we observe a marked change in the slope of the curves for shear stress ranging between 0.3 and 3 Pa, especially for GG and SH-based samples. This behavior can be probably related to the viscous drag between the polymer chains adsorbed on the CB particles and the bulk polymer, as previously described by Barrie in the case of the CB/acrylic resin composites.⁴⁸

Regarding the VES formulations, the pristine system NaOL 13% + KCl 4% shows a typical shear-thinning profile, with an extended Newtonian plateau ($\eta_0 = 230 \text{ Pa}\cdot\text{s}$) followed by a steep decrease in viscosity in the high shear stress region. This rheological behavior is ascribed to the presence of wormlike micelles,⁴⁹⁻⁵¹ that brings about a rapid drop in the viscosity due to their shear-induced alignment.⁵² It is widely reported that the addition of inorganic salts to aqueous solutions of oleate promotes the growth of spherical micelles into ‘polymer-like’ elongated aggregates, due to the screening of the electrostatic interactions between the charged headgroups.^{52,53} Above a critical concentration these wormlike micelles form an entangled network, giving rise to a viscoelastic behavior which is reminiscent of that of flexible polymer solutions.⁵⁴⁻⁵⁶

When CB is added to the VES system up to 10% w/w, the shear-thinning behavior is retained, albeit a viscosity variation from 1000 to 5000 Pa·s over the shear stress range 0.1-100 Pa. A remarkable increase in the zero-stress viscosity is detected (from 230 to 5400 Pa·s compared with the pristine VES formulation), indicating that the carbonaceous particulate acts as a reinforcing agent for the network. Furthermore, the critical stress at which the viscosity breaks down shifts to higher values, confirming the structuring effect of the CB particles.

In order to get a deeper insight into the effect of CB on the mechanical properties of NaOL dispersions, oscillatory frequency sweep tests were carried out on VES systems before and after the addition of 10% of carbon black (see Figure 4).

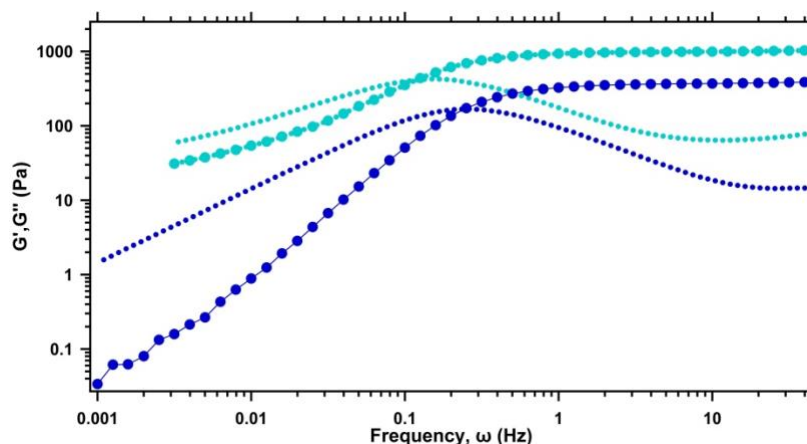


Figure 4. Storage (circles) and loss (dotted lines) moduli of pristine (dark blue) and 10% w/w CB-enriched (light blue) NaOL 13% + KCl 4% VES formulations. All the measurements were carried out in the linear viscoelastic regime (strain amplitude = 1.0 %).

The formulations exhibit the typical rheological behavior of viscoelastic fluids, with two distinct regimes. At low frequencies, when $\omega < \omega_c$ (ω is the frequency, ω_c is the crossover frequency between the two moduli) the loss modulus G'' exceeds the storage modulus G' , indicating a predominantly viscous behavior. Instead for $\omega > \omega_c$ G' dominates and the system is mainly elastic. In simple physical terms, this crossover separates the plateau regime of the collective network dynamics from the single-filament regime.⁵⁷ The dynamics of the studied systems cannot be described according to the single-element Maxwell model, hence G' and G'' are used to calculate the time-weighted relaxation spectra $H(\tau)$ reported in Figure 5.⁵⁸

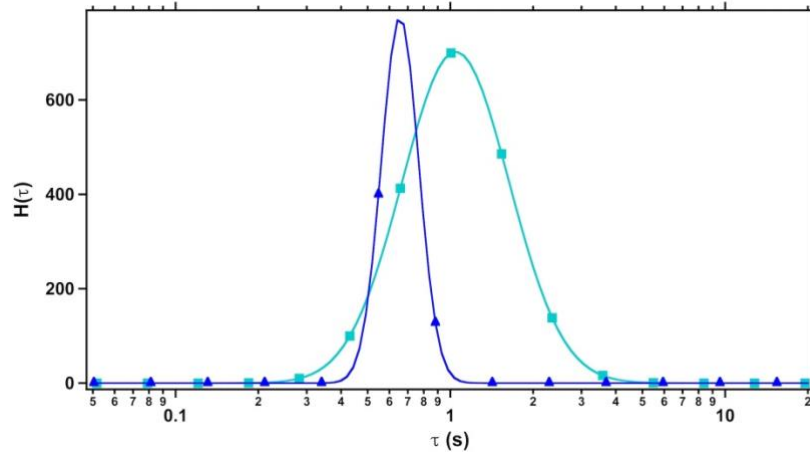


Figure 5. $H(\tau)$ relaxation spectra of pristine (dark blue) and CB-enriched (light blue) NaOL 13% + KCl 4% VES formulations.

The relaxation spectra exhibit a broad primary peak from which we estimate the relaxation times. The CB-enriched VES formulation shows a longer relaxation time, confirming the reinforcing role of CB in the stabilization of the wormlike matrix. Moreover, considering that the numbers of interconnections in the self-assembled structure is directly related to the values of the elastic plateaus in the oscillatory frequency sweep tests (Figure 5),⁵⁹ we argue that the addition of CB leads to the formation of a more entangled network, as suggested by the higher value of the G' modulus for the CB-enriched sample.

A further confirmation of the negligible effect of CB on the micellar structure of NaOL is provided by SAXS experiments (Figure 6).

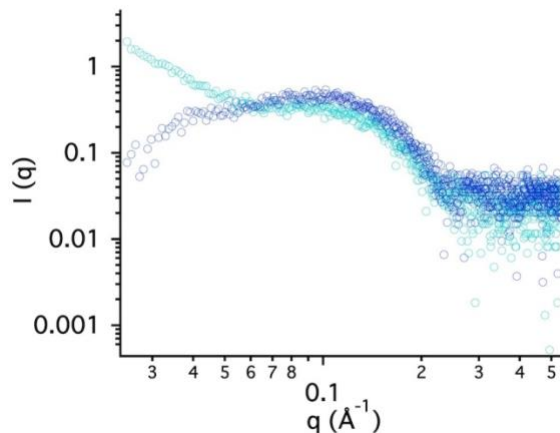


Figure 6. SAXS curves of VES formulations: NaOL 13% + KCl 4% (dark blue circles) and 10% CB enriched samples (light blue circles).

The scattering curves before and after the addition of CB are similar, except for the strong contribution to the scattering intensity in the low q -region ($q < 0.005 \text{ \AA}^{-1}$) due to the CB particles. This result points out that the dimensions of the charged aggregates and the electrostatic interactions among the elongated micelles are not affected by the addition of CB. According to the literature,^{52,53,60} the observed scattering profile is associated to the presence of polydispersed core-shell elongated objects interacting via a screened Coulomb potential in solution.

Electric responsiveness test. The application of a voltage ΔV (30 V for 1 hour) to the formulations produces electrophoretic, polarization and osmotic effects, that result in the separation of a liquid and easy-flowing phase on one electrode, and of a viscous phase that concentrates at the opposite side. The effect of the external electrical stimulus is investigated both on pristine formulations and on CB-enriched systems. Table 1 reports the mass percentage of the recovered liquid (L) and viscous (V) phases along with their zero-stress viscosities η_0

obtained from flow curve experiments. The flow curves of the polysaccharides networks after the electric treatment without CB and in the presence of 3% w/w of CB are shown in Figures S2 and S4, respectively. Figures S3 and S4 report the flow curves of pristine and CB-enriched VES formulations after the electric stimulation, respectively.

Table 1. Zero-stress viscosities for the polysaccharide and VES-based formulations before the application of the voltage (η_0 , Pa·s), mass percentage and zero-stress viscosities of liquid and viscous phases (L , V , $\eta_{0,L}$, $\eta_{0,V}$) recovered after the application of a voltage (30 V for 1 hour).

Sample	Before ΔV	After ΔV			
	η_0 (Pa·s)	L (%)	$\eta_{0,L}$ (Pa·s)	V (%)	$\eta_{0,V}$ (Pa·s)
GG	2.1	-	1.1	-	1.1
HPC	1.3	60	0.5	40	40
SH	13	52	0.1	48	43
NaOL 13% + KCl 4%	230	66	4.4	34	390
GG + CB 3%	67	-	22	-	22
HPC + CB 3%	120	50	20	50	4500
SH + CB 3%	130	30	63	70	1000
NaOL13% + KCl 4% + CB 10%	5400	-	$3.6 \cdot 10^5$	-	$3.6 \cdot 10^5$

Concerning the pure polysaccharide-based fluids, we observe that HPC and SH dispersions exhibit phase separation in response to the electric treatment, with a recovered viscous phase of about 40 – 48%. In particular, the viscous phase shows a remarkable increment in η_0 , which increases from 13 and 1.3 Pa·s to 48 and 40 Pa·s for SH and HPC, respectively, while for the liquid phase the viscosity decreases by two orders of magnitude. Despite this strong change in the viscosity of the formulation before and after the application of the voltage, the rheological profiles remain more or less unaltered, suggesting that no structural modifications or degradation in the polysaccharidic network are induced by the electric stimulation. On the contrary, the

application of the external voltage does not affect the behavior of the guar gum-based formulation, that remains in its initial homogeneous monophasic state after the treatment.

The formation of two phases with different viscosities upon the application of the voltage can be attributed to the electrically-induced differences in the polysaccharide/water volume ratio: in fact, the applied voltage leads to the contraction of the polysaccharide matrix with the consequent reduction of the mesh size and the partial removal of water from the network. Thus, the relative amount of the recovered phases after the electric stimulation strictly depends on the nature of the polysaccharide.

Similar results with the formation of two phases with different viscosity after electrostimulation are observed also for the pure NaOL-based formulation (see Figure S3). Indeed, the viscous phase collected at one electrode shows a significant increase in η_0 (from 230 to 390 Pa·s) along with a remarkable contraction of the Newtonian region and a shift of the critical stress towards lower values. The viscosity of the liquid phase decreases by two orders of magnitude, and the downward shift of the critical stress is observed also in this case. The rheological profiles of the two recovered phases significantly differ from that of the untreated fluids. This result suggests that the application of the voltage partially breaks the micellar entanglement and the self-assembled structures, leading to irregular and variable profiles in comparison to the pristine VES flow curve.

In this section, we discuss the results concerning the effect of CB addition on the electro-responsiveness of both polysaccharide and VES formulations. The mass percentage of the recovered liquid (L) and viscous (V) phases together with their zero-stress viscosities η_0 are

listed in Table 1. The flow curves of the fluids recovered after the application of the electric stimulation in the presence of CB are reported in Figure S4 in the Supporting Information.

In the case of the polysaccharide-based formulations, the relative increase in the zero-shear viscosities of the viscous phase after the electric treatment is exceptionally large compared to the pure polysaccharides, with the exception of guar gum. In particular, η_0 increases from 120 to 4500 Pa·s for HPC and from 130 to 1000 Pa·s in the case of SH formulations. These results confirm the remarkable structuring effect of CB on the polysaccharide texture and highlight its contribution to the physical phenomena (*i.e.* electrophoretic, polarization and osmotic effects) that regulate the electric response of the fluid. The CB-polymer intermolecular interactions are usually interpreted in terms of a tunneling effect,³³ a percolation phenomenon³⁴ or through a combination of the two models.^{35,36} Both models assume a close contact between the polymeric chains and the CB particles: the presence of the carbonaceous aggregates on the polymer enhances the electric conductivity of the fluid, promoting a stronger contraction of the polysaccharide network and resulting in higher viscosities after the electric treatment. These evidences are further confirmed by electric conductivity experiments (see Table S2 in the Supporting Information) that show a remarkable increase in the fluid conductivity when CB is added to the formulation.

When the voltage is applied to the CB-enriched VES formulation (see Figure S4 in the Supporting Information), the zero-stress viscosity increases of about two orders of magnitude (from $5.4 \cdot 10^3$ to $3.6 \cdot 10^5$ Pa·s), indicating the formation of a more rigid network that can be attributed to the shrinking of the self-assembled micellar aggregates. The strengthening effect of CB also prevents phase separation, which is not observed in this case. Moreover, the rheological profile of the formulation does not change significantly before and after the electric treatment,

showing the typical non-Newtonian behavior of the VES formulations. These results are a proof-of-concept and show the efficacy of combining CB with simple handling commercially available materials to obtain versatile formulations with an enhanced viscosity that can be effectively modified through the application of an external voltage. The use of a physical trigger enables also the re-utilization of the frac fluids, which can be easily recovered, regenerated or recycled for subsequential fracturing operations. Preliminary experiments demonstrate that the original viscosity and rheological properties can be restored by adding a proper amount of water to the viscous phase which is recovered at the electrode. In particular the polysaccharide-based formulations can undergo this transition 2-3 times at least, without degradation or performance loss.

Effect of temperature. Another peculiar feature of CB-enriched polymer composites is their improved thermal stability.^{61,62} To address this point, flow curves are acquired on polysaccharide and VES-based fluids at 25, 30, 40, 50, and 60 °C. The zero-stress viscosity values η_0 at the different temperatures are listed in Table 2. The flow curves as a function of T acquired on all the investigated formulations are reported in Figures S5, S6, S7 and S8 in the Supporting Information.

Table 2. Zero-stress viscosity values (η_0 , Pa·s) and the extracted Gibbs free energy of activation (ΔG^\ddagger , kJ·mol⁻¹) for polysaccharide and VES formulations before and after the addition of CB at 25, 30, 40, 50 and 60 °C.

η_0 (Pa·s)			
GG	SH	HPC	VES

T (°C)	No CB	CB	No CB	CB	No CB	CB	No CB	CB
25	2.1	67	13	130	1.3	120	230	5400
30	1.6	53	10	65	1.8	203	150	2421
40	1.3	44	8.4	34	3.1	390	36	1627
50	0.7	26	6.1	8	8.4	594	11	2985
60	0.3	10	4.9	1.7	15	805	4	3914
ΔG^\ddagger	38.9	38.8	20.8	92.4	-	-	91.5	-

Similar results are obtained in the case of the pristine GG and SH-based formulations: the raise in temperature induces a downward shift in the flow curve, with a progressive lowering of the zero shear-viscosity value as temperature increases. Indeed, the intermolecular interactions are weakened as temperature raises, resulting in a softer network where the polysaccharide chains flow with a progressively lower friction. However, no thermal degradation or irreversible modifications occur in the polymer matrix.

In the presence of CB, the viscosity decrement as a function of temperature is still evident, but the values of η_0 are significantly larger in comparison to the pure polysaccharide networks, indicating that the carbonaceous particles improve the thermal response of the formulation. It is interesting to observe that the flow curves of CB-enriched GG and SH systems exhibit a double plateau and a double drop in the flow profile (Figures S5 and S6 in the Supporting Information). This peculiar behavior suggests the formation of CB-induced ordered structures which are

responsible for the higher viscosity in the lower stress region. When the applied stress increases, these structures break down and the flow profiles overlap in the shear-thinning region. Increasing temperature, the critical stress at which the higher viscosity plateau starts to decline shifts towards lower stress values: the gap between the first and the second plateau progressively becomes less pronounced, until it is barely visible in the profile recorded at 60 °C. This result indicates that the highly ordered structure loses its stability.

A completely opposite behaviour is observed for HPC-based formulation: the zero-shear viscosity increases with temperature, indicating that the polysaccharide network becomes more viscous and rigid. Moreover, also the critical stresses corresponding to the collapse of the network are shifted to higher values. This counterintuitive response is related to the peculiar phase behavior of hydroxypropyl cellulose in water: HPC exhibits a lower critical solution temperature (LCST), and it is known to form a liquid-crystalline phase in a concentrated solution. After phase separation, the polymer-rich phase forms an anisotropic liquid-crystalline layer.⁶³ The balance between the hydrophilic and hydrophobic interactions of inter- and intrapolymer chains is essentially responsible for this phase transition in the HPC network.^{64,65} The temperature increase perturbs the interactions between water molecules and polymer chains, leading to polymer association and to the collapse of the swollen network. The formation of aggregates eventually brings about an increase of the formulation viscosity, as shown by the flow curve experiments.

Regarding the NaOL-based formulations, the temperature increase induces the breaking of the entangled micellar network with a rapid drop in the viscosity of the system in the absence of CB (see Figure S8, Supporting Information). In the case of CB-enriched formulations, the zero-shear viscosities are about two orders of magnitude higher, confirming the reinforcement of the

network due the addition of CB (see Table 2). It is also important to note that the rheological profiles obtained in the presence of CB are quite different from those of the pristine formulations, with two different regions before the drop in the shear-thinning regime (see Figure S8 in the Supporting Information). Presumably, for low shear stress values, both the self-assembled micelles and the CB particles move together with the typical Newtonian behavior. When higher shear stresses are applied to the system, the viscous force between sodium oleate micelles and the carbonaceous particles arises, producing a second region where the system behaves as a shear-thinning material.⁴⁸ It is worth noting that the system seems to have a more pronounced shear-thinning behavior as temperature increases, as suggested by the value of critical stress that corresponds to the onset of the second region. For shear stresses higher than 100 Pa, the viscosity drop is similar to that observed for the formulation without CB, indicating the total break of the entangled micellar network even in the presence of the reinforcing agent.

From a thermodynamic standpoint the trend of the low-stress plateau region at different temperatures can be investigated in terms of an activated mechanism according to a modified Arrhenius equation (further details and the Arrhenius plots are reported in Figures S9, S10, S11 in the Supporting Information).⁶⁶ The extracted Gibbs free energy of activation (ΔG^\ddagger) for the polysaccharide and VES formulations are reported in Table 2.

For the NaOL-based formulation, we obtain $\Delta G^\ddagger = 91.5 \pm 5.1 \text{ kJ}\cdot\text{mol}^{-1}$, reflecting a tight entanglement of the chains that hinders the flow. This value is in line with the previous literature.^{67,68} In the presence of CB, the VES system exhibits a different and non regular response to the temperature raise. Indeed, the viscosity decreases in the range between 25 and 40 °C, as observed in the case of pure VES, whereas it shows a higher plateau when temperature is further increased up to 50 and 60 °C.

In the case of pure aqueous SH and GG dispersions, we obtain values for ΔG^\ddagger of 20.8 ± 1.1 and 38.8 ± 5.1 $\text{kJ}\cdot\text{mol}^{-1}$, respectively. The calculated ΔG^\ddagger values of the two polysaccharide dispersions fall in the range reported in the literature for polymers.⁶⁹ A similar analysis cannot be extended to HPC because of its peculiar thermal behavior. As we already pointed out, when CB is added to the polysaccharide systems, we observed different responses to a temperature increment. In the case of GG (a neutral polymer), we obtain almost the same ΔG^\ddagger value of the same system before the addition of CB (38.9 ± 7.3 $\text{kJ}\cdot\text{mol}^{-1}$). Instead, in the case of the anionic SH, the addition of CB induces a significant change in ΔG^\ddagger , that increases up to 92.4 ± 9.6 $\text{kJ}\cdot\text{mol}^{-1}$.

4. CONCLUSIONS

Carbon black (CB) was dispersed in green aqueous polysaccharide or viscoelastic (VES) formulations in order to modify their rheological, thermal and electric properties.

Rheology experiments performed at 25 °C on pristine formulations and CB-enriched systems revealed a viscosity increase and a higher stress threshold before the network collapse upon the addition of CB, indicating that carbon black acts as a reinforcing agent for the network. In particular, the zero-stress viscosity increased of at least one order of magnitude for VES formulations and guar gum (GG) fluid, while an increase of about two orders of magnitude was observed for sodium hyaluronate (SH) and hydroxypropyl cellulose (HPC) networks. Similar experiments were performed increasing the temperature up to 60 °C to mimic the use of these formulations at high temperature in real applicative situations, for example in shale gas extraction. Our results demonstrated that the increase of temperature was responsible for a

progressive lowering of the zero shear-viscosity value due to a weakening of the intermolecular interactions between the molecules, except for hydroxypropyl cellulose, which showed the opposite thermal behavior. Nevertheless, the addition of carbon black brings about the reduction in the downward shift of the zero-stress viscosity with respect to the pristine formulations. This finding confirms the strengthening effect and the possibility to confer a higher thermal stability to the polymeric networks upon the addition of carbon black to the frac fluid.

Finally, the responsiveness of CB-enriched formulations to the application of an external voltage of 30 V was assessed through electric responsiveness tests. All systems exhibited phase separation in response to the electric treatment with the formation of two phases with different viscosities. In the case of polysaccharides, HPC and SH dispersions showed a remarkable response to the application of the electrical stimulus with a recovered viscous phase of about 50-70% respectively, while no significant effects were observed for guar gum formulation. Regarding the VES systems, the addition of carbon black conferred a structuring effect to the micellar network and the strengthening of the network prevented the phase separation upon the application of the external voltage. In fact only one phase with an increased zero-stress viscosity of about 10^5 Pa·s instead of 10^3 Pa·s of the same system before electrostimulation was collected.

It is worth noting that previous literature reported the addition of huge amounts of CB, *i.e.* about 20% w/w, in order to appreciably affect the properties of the composite material.²⁵ Our results showed an improvement of the performances of the studied formulations upon the addition of significantly lower CB concentrations (3% w/w for the polysaccharidic dispersions and 10% w/w for the VES formulations).

Our study demonstrates that the addition of electro-conducting solid particulates, such as carbon black, offers a smart alternative method to tune the physico-chemical properties of a viscoelastic formulation containing a polysaccharide matrix or a viscoelastic surfactant. This achievement can significantly widen the horizon of the potential applications of these CB-enriched formulations. For example, these enhanced smart composite materials can be efficiently used as innovative and green frac fluids with lower environmental impact with respect to the commonly used formulations whose physico-chemical properties are generally controlled through the addition of hazardous chemicals that represent an issue for the environment and public health.

ASSOCIATED CONTENT

Supporting Information

Optical micrographs of the CB-enriched polysaccharides and VES-based formulations (Figure S1), flow curves of electrically stimulated polysaccharide and VES fluids (Figure S2, S3 and S4), conductivity data (Table S1), the effect of temperature on the formulations' flow profiles (Figure S5, S6, S7 and S8) and the Arrhenius plots of polysaccharide and VES systems (Figure S9, S10 and S11). The following file is available free of charge: CB Green Paper SI.pdf

AUTHOR INFORMATION

Corresponding Author

* Phone: +39 055 4573010. Email: pierandrea.lonostro@unifi.it

Author Contributions

The manuscript was written through contributions of all authors. All authors have given approval to the final version of the manuscript.

ACKNOWLEDGMENT

The authors acknowledge funding from the European Union Horizon 2020 research and innovation program “Shale for Environment” (SXT) under grant agreement Nr. 640979.

ABBREVIATIONS

CB, carbon black; VES, viscoelastic; NaOL, sodium oleate; GG, guar gum; HPC, hydroxypropyl cellulose; SH, sodium hyaluronate; LCST, lower critical solution temperature; SAXS, small angle X-ray scattering.

REFERENCES

- (1) Gadonneix, P.; de Castro, F. B.; de Medeiros, N. F.; Drouin, R.; Jain, C. P.; Kim, Y. D.; Ferioli, J.; Nadeau, M.-J.; Sambo, A.; Teyssen, J. Survey of Energy Resources: Focus on Shale Gas. *World Energy Counc.* **2010**.
- (2) Luca Gandossi; Ulrik Von Estorff. An Overview of Hydraulic Fracturing and Other Formation Stimulation Technologies for Shale Gas Production - Update 2015. The European Commission’s science and knowledge service December 4, 2015.
- (3) Gidley, J. L. *Recent Advances in Hydraulic Fracturing*, 12th ed.; Richardson, Texas: Monograph Series, SPE., **1988**.
- (4) Howard, G. C.; Fast, C. R. Optimum Fluid Characteristics for Fracture Extension; American Petroleum Institute, 1957.
- (5) Barati, R.; Liang, J.-T. A Review of Fracturing Fluid Systems Used for Hydraulic Fracturing of Oil and Gas Wells. *J. Appl. Polym. Sci.* **2014**, *131* (16). <https://doi.org/10.1002/app.40735>.
- (6) Al-Muntasheri, G. A. A Critical Review of Hydraulic Fracturing Fluids over the Last Decade; Society of Petroleum Engineers, 2014. <https://doi.org/10.2118/169552-MS>.
- (7) Li, L.; Al-Muntasheri, G. A.; Liang, F. A Review of Crosslinked Fracturing Fluids Prepared with Produced Water. *Petroleum* **2016**, *2* (4), 313–323. <https://doi.org/10.1016/j.petlm.2016.10.001>.
- (8) Tatini, D.; Sarri, F.; Maltoni, P.; Ambrosi, M.; Carretti, E.; Ninham, B. W.; Lo Nostro, P. Specific Ion Effects in Polysaccharide Dispersions. *Carbohydr. Polym.* **2017**, *173*, 344–352. <https://doi.org/10.1016/j.carbpol.2017.05.078>.
- (9) Montgomery, C. Fracturing Fluids. *Eff. Sustain. Hydraul. Fract.* **2013**. <https://doi.org/10.5772/56192>.

- (10) Jiang, G.; Jiang, Q.; Sun, Y.; Liu, P.; Zhang, Z.; Ni, X.; Yang, L.; Wang, C. Supramolecular-Structure-Associating Weak Gel of Wormlike Micelles of Erucoylamidopropyl Hydroxy Sulfobetaine and Hydrophobically Modified Polymers. *Energy Fuels* **2017**, *31* (5), 4780–4790. <https://doi.org/10.1021/acs.energyfuels.6b03415>.
- (11) Elliott, E. G.; Ettinger, A. S.; Leaderer, B. P.; Bracken, M. B.; Deziel, N. C. A Systematic Evaluation of Chemicals in Hydraulic-Fracturing Fluids and Wastewater for Reproductive and Developmental Toxicity. *J. Expo. Sci. Environ. Epidemiol.* **2017**, *27* (1), 90–99. <https://doi.org/10.1038/jes.2015.81>.
- (12) Stringfellow, W. T.; Domen, J. K.; Camarillo, M. K.; Sandelin, W. L.; Borglin, S. Physical, Chemical, and Biological Characteristics of Compounds Used in Hydraulic Fracturing. *J. Hazard. Mater.* **2014**, *275*, 37–54. <https://doi.org/10.1016/j.jhazmat.2014.04.040>.
- (13) Vengosh, A.; Jackson, R. B.; Warner, N.; Darrah, T. H.; Kondash, A. A Critical Review of the Risks to Water Resources from Unconventional Shale Gas Development and Hydraulic Fracturing in the United States. *Environ. Sci. Technol.* **2014**, *48* (15), 8334–8348. <https://doi.org/10.1021/es405118y>.
- (14) Williams, N. J.; Kelly, P. A.; Berard, K. G.; Dore; Ethel; Emery, N. L.; Williams, C. F.; Mukhopadhyay, S. Fracturing Fluid With Low-Polymer Loading Using a New Set of Boron Crosslinkers: Laboratory and Field Studies; Society of Petroleum Engineers, 2012. <https://doi.org/10.2118/151715-MS>.
- (15) Zhang, B.; Davenport, A. H.; Whipple, L.; Urbina, H.; Barrett, K.; Wall, M.; Hutchins, R.; Mirakyan, A. A Superior, High-Performance Enzyme for Breaking Borate Crosslinked Fracturing Fluids Under Extreme Well Conditions. *SPE Prod. Oper.* **2013**, *28* (02), 210–216. <https://doi.org/10.2118/160033-PA>.
- (16) Gupta, D. V. S. V.; Carman, P. S.; Venugopal, R. A Stable Fracturing Fluid for Produced Water Applications; Society of Petroleum Engineers, 2012. <https://doi.org/10.2118/159837-MS>.
- (17) Li, L.; Saini, R.; Mai, N. High-TDS Produced Water-Based, Low-Damaging Fracturing Fluids for Applications at 300°F or Higher; Society of Petroleum Engineers, 2018. <https://doi.org/10.2118/191749-MS>.
- (18) Gupta, D. V. S.; Leshchyshyn, T. T. CO₂-Energized Hydrocarbon Fracturing Fluid: History and Field Application in Tight Gas Wells; Society of Petroleum Engineers, 2005. <https://doi.org/10.2118/95061-MS>.
- (19) Cao, P.-F.; Mangadlao, J. D.; Advincula, R. C. Stimuli-Responsive Polymers and Their Potential Applications in Oil-Gas Industry. *Polym. Rev.* **2015**, *55* (4), 706–733. <https://doi.org/10.1080/15583724.2015.1040553>.
- (20) Yegin, C.; Zhang, M.; Talari, J. V.; Akbulut, M. Novel Hydraulic Fracturing Fluids with Improved Proppant Carrying Capacity and PH-Adjustable Proppant Deposition Behavior. *J. Pet. Sci. Eng.* **2016**, *145*, 600–608. <https://doi.org/10.1016/j.petrol.2016.06.033>.
- (21) Ahn, S.; Kasi, R. M.; Kim, S.-C.; Sharma, N.; Zhou, Y. Stimuli-Responsive Polymer Gels. *Soft Matter* **2008**, *4* (6), 1151–1157. <https://doi.org/10.1039/B714376A>.
- (22) Wei, M.; Gao, Y.; Li, X.; Serpe, M. J. Stimuli-Responsive Polymers and Their Applications. *Polym. Chem.* **2016**, *8* (1), 127–143. <https://doi.org/10.1039/C6PY01585A>.
- (23) Jung, H. B.; Carroll, K. C.; Kabilan, S.; Heldebrant, D. J.; Hoyt, D.; Zhong, L.; Varga, T.; Stephens, S.; Adams, L.; Bonneville, A.; et al. Stimuli-Responsive/Rheoreversible Hydraulic Fracturing Fluids as a Greener Alternative to Support Geothermal and Fossil

- Energy Production. *Green Chem.* **2015**, *17* (5), 2799–2812. <https://doi.org/10.1039/C4GC01917B>.
- (24) Zhang, Y.; Kong, W.; An, P.; He, S.; Liu, X. CO₂/pH-Controllable Viscoelastic Nanostructured Fluid Based on Stearic Acid Soap and Bola-Type Quaternary Ammonium Salt <https://pubs.acs.org/doi/abs/10.1021/acs.langmuir.5b04459> (accessed Nov 28, 2018). <https://doi.org/10.1021/acs.langmuir.5b04459>.
- (25) Manchado, M. A. L.; Valentini, L.; Biagiotti, J.; Kenny, J. M. Thermal and Mechanical Properties of Single-Walled Carbon Nanotubes–Polypropylene Composites Prepared by Melt Processing. *Carbon* **2005**, *43* (7), 1499–1505. <https://doi.org/10.1016/j.carbon.2005.01.031>.
- (26) Harris, P. J. F. New Perspectives on the Structure of Graphitic Carbons. *Crit. Rev. Solid State Mater. Sci.* **2005**, *30* (4), 235–253. <https://doi.org/10.1080/10408430500406265>.
- (27) Quan, Y.; Liu, Q.; Zhang, S.; Zhang, S. Comparison of the Morphology, Chemical Composition and Microstructure of Cryptocrystalline Graphite and Carbon Black. *Appl. Surf. Sci.* **2018**, *445*, 335–341. <https://doi.org/10.1016/j.apsusc.2018.03.182>.
- (28) Liu, M.; Horrocks, A. R. Effect of Carbon Black on UV Stability of LLDPE Films under Artificial Weathering Conditions. *Polym. Degrad. Stab.* **2002**, *75* (3), 485–499. [https://doi.org/10.1016/S0141-3910\(01\)00252-X](https://doi.org/10.1016/S0141-3910(01)00252-X).
- (29) Zhao, J.; Dai, K.; Liu, C.; Zheng, G.; Wang, B.; Liu, C.; Chen, J.; Shen, C. A Comparison between Strain Sensing Behaviors of Carbon Black/Polypropylene and Carbon Nanotubes/Polypropylene Electrically Conductive Composites. *Compos. Part Appl. Sci. Manuf.* **2013**, *48*, 129–136. <https://doi.org/10.1016/j.compositesa.2013.01.004>.
- (30) Wypych, G. *PVC Degradation and Stabilization*; Elsevier, 2015.
- (31) Katz, H. S.; Mileski, J. V. *Handbook Of Fillers For Plastics*; Springer Science & Business Media, 1987.
- (32) Cao, Q.; Song, Y.; Tan, Y.; Zheng, Q. Conductive and Viscoelastic Behaviors of Carbon Black Filled Polystyrene during Annealing. *Carbon* **2010**, *48* (15), 4268–4275. <https://doi.org/10.1016/j.carbon.2010.07.036>.
- (33) Sichel, E. K.; Gittleman, J. I.; Sheng, P. Transport Properties of the Composite Material Carbon-Poly(Vinyl Chloride). *Phys. Rev. B* **1978**, *18* (10), 5712–5716. <https://doi.org/10.1103/PhysRevB.18.5712>.
- (34) Reboul, J.-P.; Moussalli, G. About Some D-C Conduction Processes in Carbon Black Filled Polymers. *Int. J. Polym. Mater. Polym. Biomater.* **1976**, *5* (1–2), 133–146. <https://doi.org/10.1080/00914037608072394>.
- (35) Balberg, I. A Comprehensive Picture of the Electrical Phenomena in Carbon Black–Polymer Composites. *Carbon* **2002**, *40* (2), 139–143. [https://doi.org/10.1016/S0008-6223\(01\)00164-6](https://doi.org/10.1016/S0008-6223(01)00164-6).
- (36) Carmona, F.; Mouney, C. Temperature-Dependent Resistivity and Conduction Mechanism in Carbon Particle-Filled Polymers. *J. Mater. Sci.* **1992**, *27* (5), 1322–1326. <https://doi.org/10.1007/BF01142046>.
- (37) Das, D.; Panigrahi, S.; Misra, P. K.; Nayak, A. Effect of Organized Assemblies. Part 4. Formulation of Highly Concentrated Coal–Water Slurry Using a Natural Surfactant. *Energy Fuels* **2008**, *22* (3), 1865–1872. <https://doi.org/10.1021/ef7006563>.
- (38) Das, D.; Panigrahi, S.; Senapati, P. K.; Misra, P. K. Effect of Organized Assemblies. Part 5: Study on the Rheology and Stabilization of a Concentrated Coal–Water Slurry Using

- Saponin of the Acacia Concinna Plant. *Energy Fuels* **2009**, *23* (6), 3217–3226. <https://doi.org/10.1021/ef800915y>.
- (39) Blanton, T. N.; Huang, T. C.; Toraya, H.; Hubbard, C. R.; Robie, S. B.; Louër, D.; Göbel, H. E.; Will, G.; Gilles, R.; Raftery, T. JCPDS—International Centre for Diffraction Data Round Robin Study of Silver Behenate. A Possible Low-Angle X-Ray Diffraction Calibration Standard. *Powder Diffr.* **1995**, *10* (2), 91–95. <https://doi.org/10.1017/S0885715600014421>.
- (40) Huang, J.-C. Carbon Black Filled Conducting Polymers and Polymer Blends. *Adv. Polym. Technol.* **2002**, *21* (4), 299–313. <https://doi.org/10.1002/adv.10025>.
- (41) Bigg, D. M. An Investigation of the Effect of Carbon Black Structure, Polymer Morphology, and Processing History on the Electrical Conductivity of Carbon-Black-Filled Thermoplastics. *J. Rheol.* **1984**, *28* (5), 501–516. <https://doi.org/10.1122/1.549758>.
- (42) Liang, F.; Chen, B. A Review on Biomedical Applications of Single-Walled Carbon Nanotubes <https://www.ingentaconnect.com/content/ben/cmc/2010/00000017/00000001/art00002> (accessed Oct 24, 2018). <https://doi.org/info:doi/10.2174/092986710789957742>.
- (43) Cataldo, F.; Ros, T. da. *Medicinal Chemistry and Pharmacological Potential of Fullerenes and Carbon Nanotubes*; Springer Science & Business Media, 2008.
- (44) Tiarks, F.; Landfester, K.; Antonietti, M. Silica Nanoparticles as Surfactants and Fillers for Latexes Made by Miniemulsion Polymerization. *Langmuir* **2001**, *17* (19), 5775–5780. <https://doi.org/10.1021/la010445g>.
- (45) Tiarks, F.; Landfester, K.; Antonietti, M. Encapsulation of Carbon Black by Miniemulsion Polymerization. *Macromol. Chem. Phys.* **2001**, *202* (1), 51–60. [https://doi.org/10.1002/1521-3935\(20010101\)202:1<51::AID-MACP51>3.0.CO;2-J](https://doi.org/10.1002/1521-3935(20010101)202:1<51::AID-MACP51>3.0.CO;2-J).
- (46) Sis, H.; Birinci, M. Effect of Nonionic and Ionic Surfactants on Zeta Potential and Dispersion Properties of Carbon Black Powders. *Colloids Surf. Physicochem. Eng. Asp.* **2009**, *341* (1), 60–67. <https://doi.org/10.1016/j.colsurfa.2009.03.039>.
- (47) Wang, W.; Efrima, S.; Regev, O. Directing Oleate Stabilized Nanosized Silver Colloids into Organic Phases. *Langmuir* **1998**, *14* (3), 602–610. <https://doi.org/10.1021/la9710177>.
- (48) C. L. Barrie; Griffiths, P. C.; Abbott, R. J.; Grillo, I.; Kudryashov, E.; Smyth, C. Rheology of Aqueous Carbon Black Dispersions. *J. Colloid Interface Sci.* **2004**, *272* (1), 210–217. <https://doi.org/10.1016/j.jcis.2003.12.004>.
- (49) Cao, Q.; Yu, L.; Zheng, L.-Q.; Li, G.-Z.; Ding, Y.-H.; Xiao, J.-H. Rheological Properties of Wormlike Micelles in Sodium Oleate Solution Induced by Sodium Ion. *Colloids Surf. Physicochem. Eng. Asp.* **2008**, *312* (1), 32–38. <https://doi.org/10.1016/j.colsurfa.2007.06.024>.
- (50) Kalur, G. C.; Raghavan, S. R. Anionic Wormlike Micellar Fluids That Display Cloud Points: Rheology and Phase Behavior. *J. Phys. Chem. B* **2005**, *109* (18), 8599–8604. <https://doi.org/10.1021/jp044102d>.
- (51) Schubert, B. A.; Kaler, E. W.; Wagner, N. J. The Microstructure and Rheology of Mixed Cationic/Anionic Wormlike Micelles. *Langmuir* **2003**, *19* (10), 4079–4089. <https://doi.org/10.1021/la020821c>.
- (52) Dreiss, C. A. Wormlike Micelles: Where Do We Stand? Recent Developments, Linear Rheology and Scattering Techniques. *Soft Matter* **2007**, *3* (8), 956–970. <https://doi.org/10.1039/B705775J>.

- (53) Flood, C.; Dreiss, C. A.; Croce, V.; Cosgrove, T.; Karlsson, G. Wormlike Micelles Mediated by Polyelectrolyte. *Langmuir* **2005**, *21* (17), 7646–7652. <https://doi.org/10.1021/la050326r>.
- (54) Clausen, T. M.; Vinson, P. K.; Minter, J. R.; Davis, H. T.; Talmon, Y.; Miller, W. G. Viscoelastic Micellar Solutions: Microscopy and Rheology. *J. Phys. Chem.* **1992**, *96* (1), 474–484. <https://doi.org/10.1021/j100180a086>.
- (55) Hassan, P. A.; Raghavan, S. R.; Kaler, E. W. Microstructural Changes in SDS Micelles Induced by Hydrotropic Salt. *Langmuir* **2002**, *18* (7), 2543–2548. <https://doi.org/10.1021/la011435i>.
- (56) Colby, R. H. Structure and Linear Viscoelasticity of Flexible Polymer Solutions: Comparison of Polyelectrolyte and Neutral Polymer Solutions. *Rheol. Acta* **2010**, *49* (5), 425–442. <https://doi.org/10.1007/s00397-009-0413-5>.
- (57) Buchanan, M.; Atakhorrami, M.; Palierne, J. F.; MacKintosh, F. C.; Schmidt, C. F. High-Frequency Microrheology of Wormlike Micelles. *Phys. Rev. E* **2005**, *72* (1), 011504. <https://doi.org/10.1103/PhysRevE.72.011504>.
- (58) Carretti, E.; Matarrese, C.; Fratini, E.; Baglioni, P.; Dei, L. Physicochemical Characterization of Partially Hydrolyzed Poly(Vinyl Acetate)–Borate Aqueous Dispersions. *Soft Matter* **2014**, *10* (25), 4443–4450. <https://doi.org/10.1039/C4SM00355A>.
- (59) Schubert, B. A.; Kaler, E. W.; Wagner, N. J. The Microstructure and Rheology of Mixed Cationic/Anionic Wormlike Micelles - Langmuir (ACS Publications). *Langmuir* **2003**, *19* (10), 4079–4089.
- (60) Dreiss, C. A.; Feng, Y. *Wormlike Micelles: Advances in Systems, Characterisation and Applications*; Royal Society of Chemistry, 2017.
- (61) Zhang, J.; Feng, S.; Ma, Q. Kinetics of the Thermal Degradation and Thermal Stability of Conductive Silicone Rubber Filled with Conductive Carbon Black. *J. Appl. Polym. Sci.* **2003**, *89* (6), 1548–1554. <https://doi.org/10.1002/app.12277>.
- (62) Yang, H.; Gong, J.; Wen, X.; Xue, J.; Chen, Q.; Jiang, Z.; Tian, N.; Tang, T. Effect of Carbon Black on Improving Thermal Stability, Flame Retardancy and Electrical Conductivity of Polypropylene/Carbon Fiber Composites. *Compos. Sci. Technol.* **2015**, *113*, 31–37. <https://doi.org/10.1016/j.compscitech.2015.03.013>.
- (63) Penfield, K. A Look behind the Salt Curve: The Link between Rheology, Structure, and Salt Content in Shampoo Formulations. *Int. J. Cosmet. Sci.* **2005**, *27* (5), 300–300. https://doi.org/10.1111/j.0142-5463.2005.00278_5.x.
- (64) Lu, X.; Hu, Z.; Gao, J. Synthesis and Light Scattering Study of Hydroxypropyl Cellulose Microgels. *Macromolecules* **2000**, *33* (23), 8698–8702. <https://doi.org/10.1021/ma000776k>.
- (65) Mithra K.; Santripi Khandai; Sidhartha S. Jena. Effect of Electrolytes on Colloidal Stability and Swelling of Hydroxypropyl Cellulose Microgels. *AIP Conf. Proc.* **2016**, *1728* (1), 020220. <https://doi.org/10.1063/1.4946271>.
- (66) Chandler, H. D. Activation Energy and Entropy for Viscosity of Wormlike Micelle Solutions. *J. Colloid Interface Sci.* **2013**, *409* (Supplement C), 98–103. <https://doi.org/10.1016/j.jcis.2013.07.054>.
- (67) Kuryashov, D. A.; Philippova, O. E.; Molchanov, V. S.; Bashkirtseva, N. Y.; Diyarov, I. N. Temperature Effect on the Viscoelastic Properties of Solutions of Cylindrical Mixed

- Micelles of Zwitterionic and Anionic Surfactants. *Colloid J.* **2010**, 72 (2), 230–235. <https://doi.org/10.1134/S1061933X10020134>.
- (68) Angelescu, D.; Khan, A.; Caldararu, H. Viscoelastic Properties of Sodium Dodecyl Sulfate with Aluminum Salt in Aqueous Solution. *Langmuir* **2003**, 19 (22), 9155–9161. <https://doi.org/10.1021/la034770a>.
- (69) Desbrieres, J. Viscosity of Semiflexible Chitosan Solutions: Influence of Concentration, Temperature, and Role of Intermolecular Interactions. *Biomacromolecules* **2002**, 3 (2), 342–349. <https://doi.org/10.1021/bm010151+>.